BMC Musculoskeletal Disorders

RESEARCH

Open Access

Elbow rotation affects the accuracy of rotational formulas: validation of a modified method

Yong Liu[1,3†], Xiaoju Liang[1†], Jianping Sun[1], Jining Qu[1], Bohai Qi[1], Yating Yang[1,2] and Qiang Jie[1,2*]

Abstract

Background Supracondylar humerus fractures (SCHFs) are the most common elbow fractures in children and are typically treated with closed reduction and Kirschner pin fixation. However, varying degrees of residual rotational displacement may remain after closed reduction. Several methods exist to assess rotational displacement, but none account for the effect of elbow rotation on the results. We hypothesize that the accuracy of the primitive rotational calculation formula (PRCF) decreases as elbow rotation increases and propose a modified rotational calculation formula (MRCF). This study aims to investigate the impact of elbow rotation on PRCF and validate the reliability of MRCF.

Methods Mimics software was used to reconstruct the distal humerus in a child and create a transverse SCHF, which was then subjected to X-ray fluoroscopy simulation. Axial rotational displacement was simulated in 5° increments, from 0° to 45°. Internal and external elbow rotations were simulated by adjusting the "LAO" and "RAO" angles. Five physicians measured and calculated displacement using both the primitive and modified rotational calculation formulas.

Results The PRCF method showed an average error of 17.98° ± 12.31° with a maximum error of 46.46%. Additionally, 13% of measurements had an error under 3°, and 29% had an error under 10°. With MRCF, the mean error for internal rotation was 2.04° ± 1.67°, with a maximum of 6.09%; 68% of cases had an error under 3° and 94% under 5%. For external rotation, the mean error was 2.74° ± 2.66°, with a maximum of 8.29%; 57% of cases had an error under 3° and 98% under 8°. Intraclass correlation coefficients for the five physicians were 0.966 for internal rotation and 0.989 for external rotation.

Conclusions This study demonstrates that the accuracy of PRCF decreases as elbow rotation increases, supporting our hypothesis. MRCF effectively addresses the limitations of PRCF and provides stable, accurate measurements of rotational displacement even with varying elbow rotations. Accurate assessment of rotational displacement in the horizontal plane is essential to understanding the relationship between residual rotational displacement and SCHF prognosis. MRCF will play a critical role in this process.

†Yong Liu and Xiaoju Liang contributed equally to this work.

*Correspondence:
Qiang Jie
jieqiangchina@126.com

Full list of author information is available at the end of the article

Keywords Supracondylar humerus fractures, Rotational displacement, Kirschner wire fixation, 3D fluoroscopy simulation, Rotational calculation

Background

Supracondylar humerus fractures (SCHF) are the most prevalent upper limb fractures in children. Percutaneous internal fixation using Kirschner wires with closed reduction is the standard treatment. Despite this, fractures frequently remain rotationally or horizontally displaced to varying extents post-surgery [1, 2]. However, there is currently no evidence that rotational displacement of the distal fragment in the horizontal plane can spontaneously remodel or correct [3–6]. Moreover, the impact of horizontal plane rotational displacement on the functional recovery of the elbow joint remains unclear [7, 8]. Residual rotational displacement may also lead to elbow varus deformity, ulnar neuritis, and other complications [9–12]. Therefore, to elucidate the relationship between the degree of residual rotational displacement and the prognosis of SCHF, it is crucial to accurately assess rotational displacement in the horizontal plane.

Several methods have been proposed to assess horizontal rotational displacement, including the lateral rotation percentage (LRP), rotation calculation formula, and rotation calculation model [13–15]. Accurate measurement requires standard fluoroscopic positioning of the affected limb. However, obtaining standard fluoroscopic films is particularly challenging in children [16]. Clinically, after fracture confirmation, temporary splints, braces, or casts are used to immobilize the limb, preventing further displacement and protecting soft tissues and nerves. However, these materials can hinder standard fluoroscopic positioning. Additionally, young children often struggle with pain and discomfort, leading to low compliance and resistance during repeated limb adjustments. These adjustments not only increase pain but also complicate fluoroscopy, promote fracture displacement, and elevate the risk of peripheral vascular and nerve damage.

The primitive rotational calculation formula proposed by Henderson shows relative accuracy in assessing residual rotational displacement [13]. However, its sensitivity to elbow rotation is unclear, indicating a need for a more generalizable method to quantify and evaluate rotational displacement.

This study utilized three-dimensional (3D) software for biomechanical simulations of SCHF to overcome the limitations of repeated clinical fluoroscopy and uncontrolled rotational displacement. Mimics software was used to simulate rotational displacement, offering controllable conditions and reducing errors from manual adjustments. The study aims to evaluate the effect of elbow rotation on the accuracy of the primitive rotational calculation formula (PRCF) and the modified rotational calculation formula method (MRCF) for horizontal rotation shift by reconstructing various rotational states and simulating perspectives through 3D software.

Methods

Acquisition of raw data

This study retrospectively reviewed the imaging data of children aged 5–7 years who underwent spiral computed tomography (CT) scans of the elbow at Xi'an Honghui Hospital in June 2023 [17]. To ensure optimal imaging quality, all CT scans were performed by radiologic technologists with over three years of professional experience, using a Philips 64-slice CT scanner. Standardized parameters were applied (voltage: 120 kV; current: 181 mA; slice thickness: 1 mm) to maintain consistency and accuracy in the imaging process. Parental or legal guardian consent for participation was obtained for all participants, including those under the age of 16, in accordance with the ethical guidelines of Xi'an Honghui Hospital. The study was approved by the hospital's ethics committee.

Inclusion criteria were as follows: (1) The CT scan encompassed the entire distal humerus; (2) The distal humerus was free from fractures, lesions, and metallic objects within the scan range. Exclusion criteria included: (1) Presence of artifacts or low resolution; (2) Previous fractures or post-healing changes in the distal humerus; (3) Other congenital developmental abnormalities.

After applying these inclusion and exclusion criteria, a random child's DICOM data was selected as the basis for Mimics modeling. Personal information was removed, and the images were exported in DICOM format and stored on a CD.

Model construction and medical X-ray simulation

The DICOM files were processed using Mimics software (version 21.0, Materialise) for reslicing to correct positional changes during spiral CT scanning, realigning the anterior-posterior (AP) and lateral views of the humerus for modeling elbow rotation. After reslicing, the bone blocks were reconstructed, and the distal humerus block was isolated from non-humeral structures, retaining only the distal humerus model.

A transverse SCHF was artificially created, positioning the fracture line at the midpoint of the olecranon fossa's longitudinal axis. The humerus was divided into proximal and distal segments at the fracture line, and two points along the humeral mid-axis were chosen as the rotation axis. The proximal humerus was fixed, while the distal humeral block was rotated internally along the mid-axis

using the "Reposition" function in "Align." Previous research indicated that rotational displacement of the distal and proximal fragments becomes clinically significant when visible on fluoroscopy at 30° [14].

To explore different degrees of rotational displacement, the study increased displacement up to 45°, with 5° increments from 0° to 45° [14, 18]. This simulated the rotational displacement of the distal and proximal fracture fragments. The model was then used in the "Fluoroscopy" simulation. The "Distance source to detector" was set to 1000 mm, the "Distance source to patient" to 500 mm, and the "Contrast" for the bone fragments was set to 1. The resolution was set to "Hi" (600×600) to enhance the cortical edge visibility (Fig. 1). Internal and external elbow rotations were simulated by adjusting "LAO" and "RAO" angles, with increments of 5° from 0° to 45°.

Measurement and calculation formula for rotational operations

The widths of the proximal "X" and distal "Y" fracture blocks at the fracture line level were measured for each simulated film (Fig. 2). The standard AP and lateral widths in the absence of elbow rotation or displacement were labeled as "A" and "B" (Fig. 1). The standard lateral view was determined by observing the tear-drop pattern of the distal humerus, while the AP view was rotated 90° from this lateral position [16].

To assess the effect of varying degrees of elbow rotation on PRCF measurements, an AP view of the humerus was used as the measurement plane, as outlined in Henderson's paper. In contrast, MRCF required consideration of the direction of humeral rotation, so the left lateral view was chosen for measurement.

Primitive rotation calculation formulas (PRCF)

$$a = \arccos\left(\frac{Y-B}{X-B}\right) \tag{1}$$

Modified rotation calculation formulae (MRCF)

PRCF fails to consider the impact of elbow rotation. MRCF aims to compare the morphology of the distal and proximal fracture blocks in the rotated state with that of the distal and proximal fracture blocks in the standard lateral position, respectively, in order to determine the degree of rotational displacement between the bone blocks (Fig. 3). The following formulae were derived:

$$\begin{cases} \alpha_1 = \left\{90 - \left|arccos\left(\frac{X-B}{A-B}\right)\right|\right\} \times (\pm 1) \\ \alpha_2 = \left\{90 - \left|arccos\left(\frac{Y-B}{A-B}\right)\right|\right\} \times (\pm 1) \end{cases} \tag{2}$$

- The default internal rotation is positive and is multiplied by 1 for inward rotation and – 1 for outward rotation.
- α1 represents the degree of rotation of the proximal fracture block under rotational displacement relative to non-rotational displacement.
- α2 represents the degree of rotation of the distal fracture block under rotational displacement relative to non-rotational displacement.

$$\alpha = |\alpha_1 - \alpha_2|$$

- The degree of rotational displacement between the distal and proximal fracture blocks is designated by the symbol α.

The degree of rotational displacement was measured using Mimics software by a senior imaging physician and five orthopedic surgeons (three pediatric specialists and two medical students). The lengths of the distal and proximal bone fragments at the fracture line were assessed using the "line" tool in the "ANALYZE" function. Initially, the senior imaging physician took three measurements of all data, with the average used as the final result. The five other doctors independently measured the simulated films, blinded to the initial results. A separate doctor, uninvolved in the measurements, calculated the degree

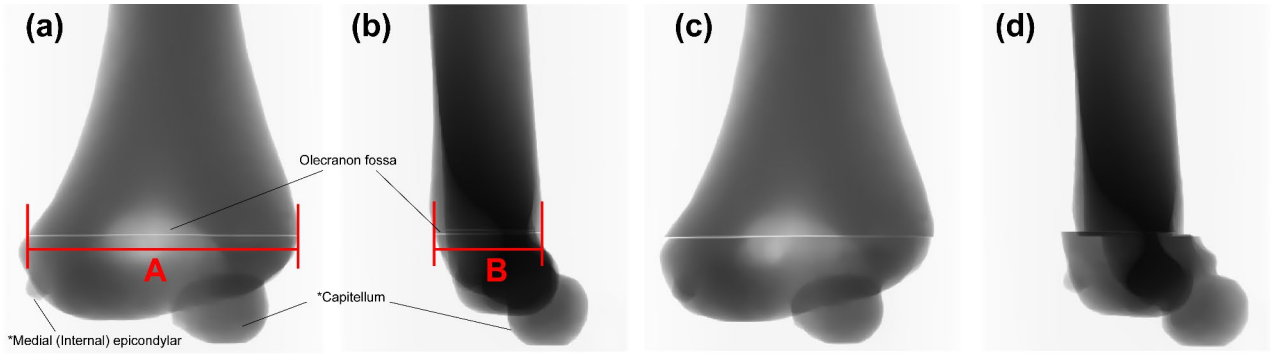

Fig. 1 (**a**) Simulated Anteroposterior Fluoroscopy Image, with A indicating the length of the humerus at the fracture level under this projection. (**b**) Simulated Lateral Fluoroscopy Image, with B indicating the length at the fracture level under this projection. (**c**) Simulated Anteroposterior Fluoroscopy Image with 15° Rotation. (**d**) Simulated Lateral Fluoroscopy Image with 15° Rotation. (*Ossification centers)

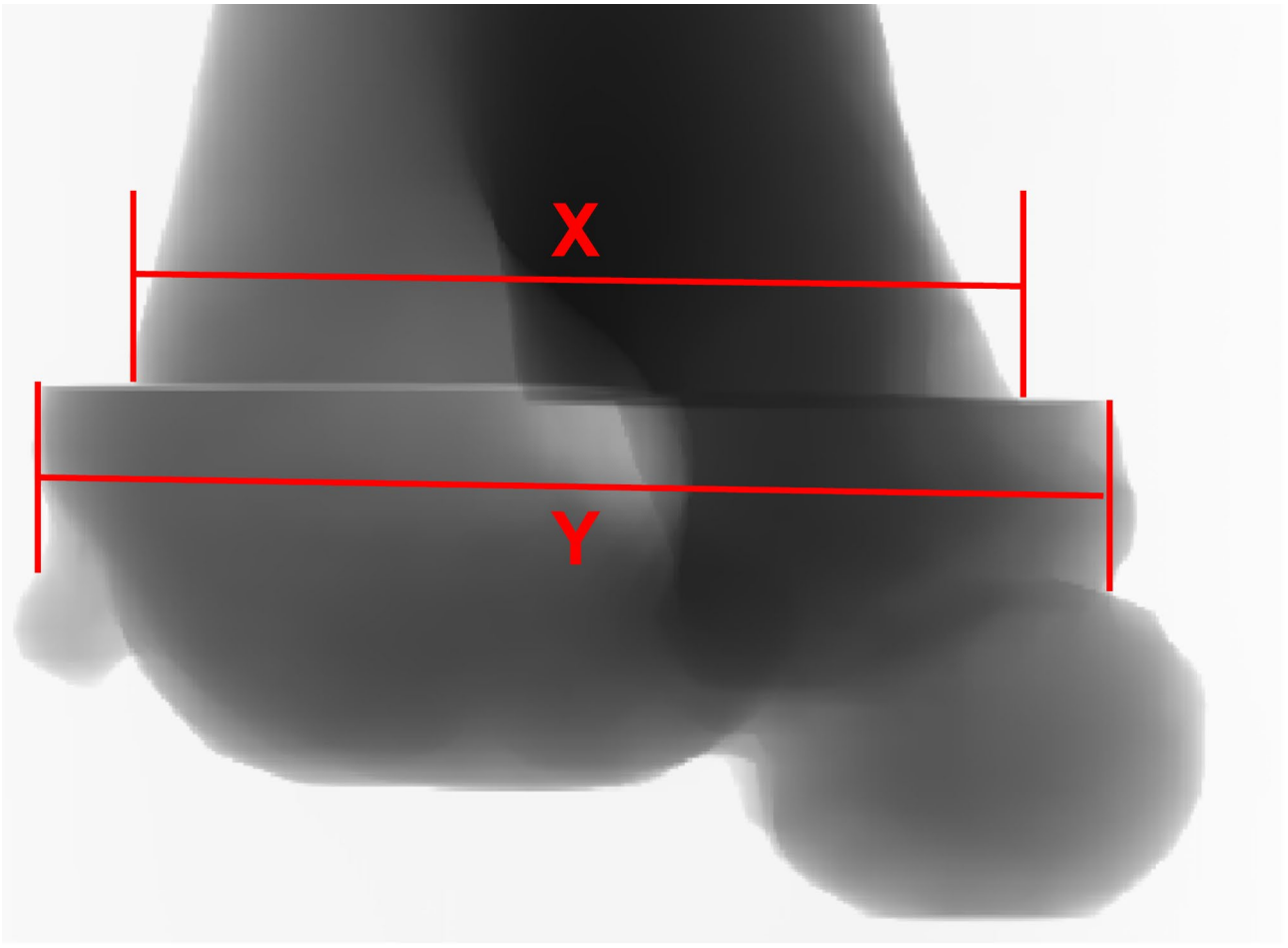

Fig. 2 Simulated Fluoroscopy Image of 15° Relative Rotational Displacement of Proximal and Distal Bone Fragments with 30° Internal Rotation of the Elbow. X is the width of the proximal humerus at the fracture level. Y is the width of the distal humerus at the fracture level

of rotation using different formulas, and the data underwent statistical analysis.

Statistical analysis

Data were compiled and analyzed in Microsoft Excel (Microsoft 365) with statistical and graphical outputs generated using GraphPad Prism (version 9.5). The rotational displacement of the bone block under various elbow rotation states was calculated using PRCF and MRCF, and the differences between the measured and true values were recorded as error values. The percentage of measurement groups falling within error ranges from 3° to 10° was calculated, and box plots displayed the distribution of errors, including mean, maximum, and minimum values. Line plots showed the variation in error percentage across different elbow rotations, while bar graphs depicted the overall percentage of error. The inter-rater reliability was evaluated using the intraclass correlation coefficient (ICC).

Results

The study concluded with the creation of a model and the use of simulated fluoroscopy on the distal humerus of a six-year-old child. A total of 200 simulated films of internal rotation of the distal humeral fracture block in the supracondylar humerus at 0–45° were obtained in the 0–45° elbow internal and external rotation states. Each elbow rotational state was accompanied by 10 measurement groups of different distal humerus blocks displaced inwardly in rotation, for a total of 100 measurement groups combining the elbow internal and external rotation groups.

Primitive rotation calculation formula's output is influenced by elbow rotation

The rotational displacement measurements of the bone block under varying degrees of elbow rotation, calculated using PRCF in AP fluoroscopy, are shown in Fig. 4a. Figure 4b illustrates the error distribution across different elbow rotations. A positive correlation between the measurements and true rotation values was observed,

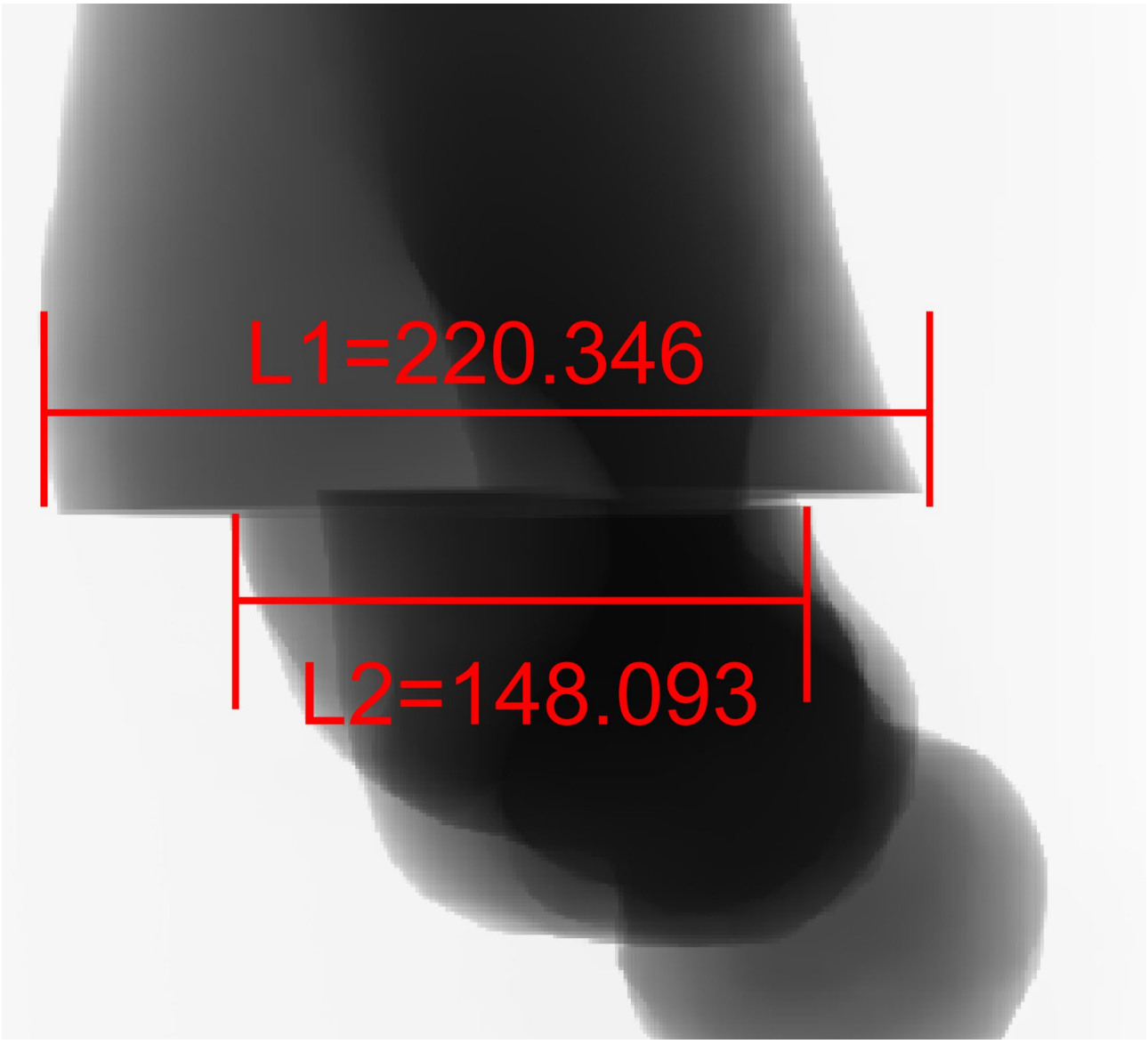

Fig. 3 Example of a simulated fluoroscopic view showing the calculation of rotational displacement between bone fragments in a scenario of elbow rotation. The elbow is externally rotated by 23°, and the true rotational displacement between the bone fragments is 20° of internal rotation. The fracture-level widths of the proximal (L1 = 220.346) and distal (L2 = 148.093) bone fragments were measured using Mimics software. Additionally, standard antero-posterior (AP) and lateral views were obtained for comparison, with AP width (**A**) = 364.10 and lateral width (**B**) = 144.05. Using the Modified Rotational Calculation Formula (MRCF), the calculated rotational displacement was 21.33°, which is only 1.33° different from the true rotational displacement of 20°. This example highlights the precision of the method in determining rotational displacement, even under different degrees of elbow rotation

but discrepancies increased with greater internal elbow rotation. In the internal rotation group, the average error between the measured and true values was 17.98° ± 12.31°, with a maximum error of 46.46°. The percentage of error in different error ranges showed a gradual decreasing trend (Fig. 4c). At 0° elbow rotation, the discrepancy between the true and measured values was minimal, with 40% of measurements showing an error within 3°. In 13% of cases, the error was less than 3°, and in 29%, it was under 10% (Fig. 4d).

Application of modified rotational calculation formula

The calculated values for rotational displacement under varying degrees of internal and external elbow rotation, obtained using MRCF in lateral fluoroscopy, are shown in Fig. 5a. Error distributions are displayed in Fig. 5b. MRCF showed less sensitivity to elbow rotation compared to PRCF. The mean error for internal rotation was 2.04° ± 1.67°, with a maximum error of 6.09°, while external rotation showed a mean error of 2.74° ± 2.66°, with a maximum error of 8.29°. Figure 6a illustrates the effect of elbow rotation on error percentages, while Fig. 6b

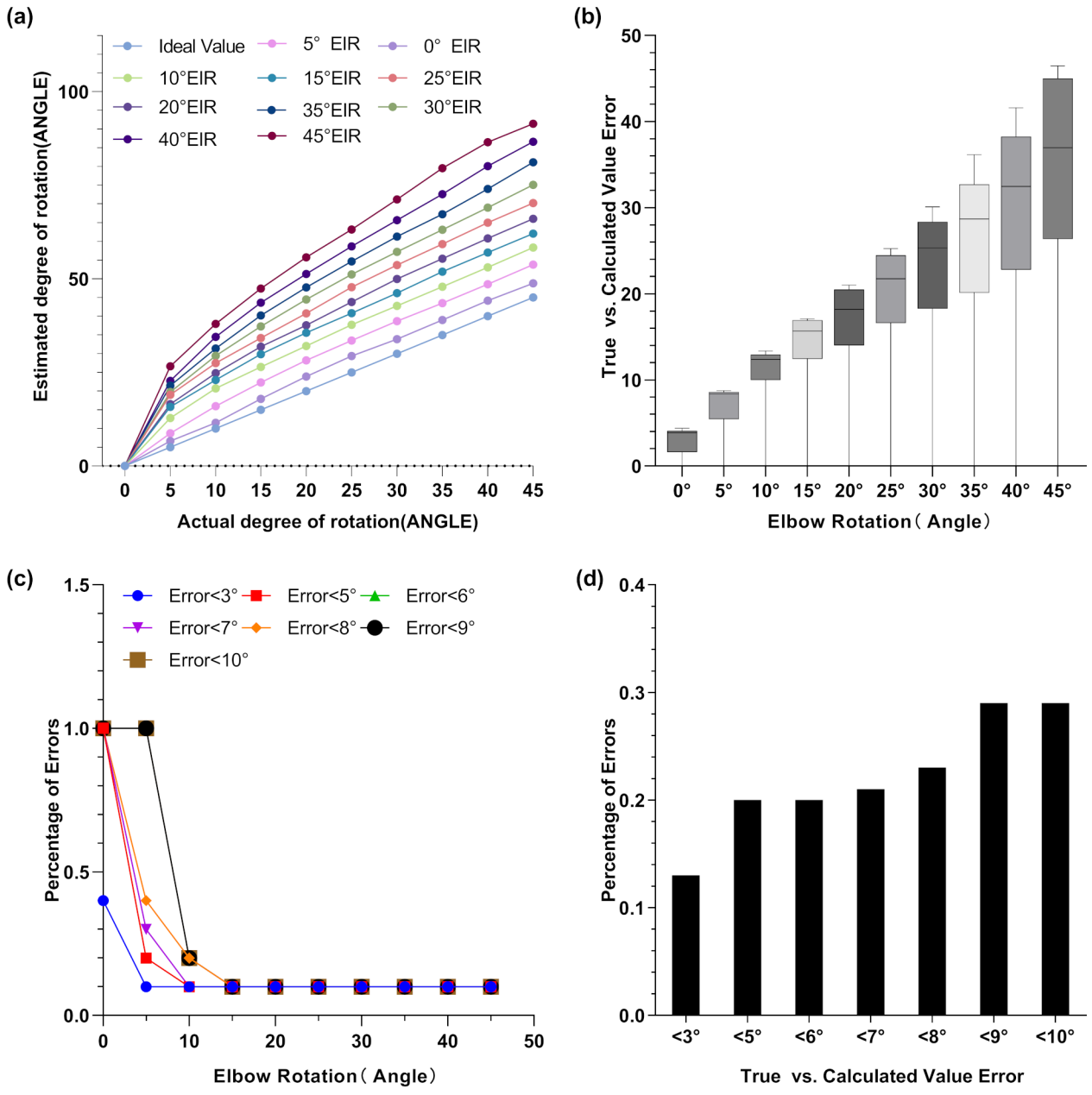

Fig. 4 (**a**) Measurements using the primitive rotation correction formula (PRCF) at varying degrees of elbow internal rotation (EIR). (**b**) Box plots showing discrepancies between measured and actual values across different EIR angles using PRCF. (**c**) Percentage error at different degrees of EIR, calculated using PRCF. (**d**) Overall percentage distribution of error levels across all measurement groups using PRCF

presents the overall percentage of error across all groups. In internal rotation, 68% of measurements had errors under 3°, 94% had errors under 5°, and all had errors below 7°. For external rotation, 57% had errors under 3°, 98% were below 8°, and all were below 9°. The assessment reliability by five physicians was excellent, with ICCs of 0.966 for internal and 0.989 for external rotation.

Discussion

This study demonstrates that elbow rotation significantly affects the stability and accuracy of rotational displacement assessments using Henderson's rotational calculation formula. In contrast, the modified formula we propose is less influenced by elbow rotation, providing more stable and reliable results. Specifically, as the degree of internal elbow rotation increases, the accuracy of the Henderson method decreases, leading to greater measurement error. The improved evaluation method

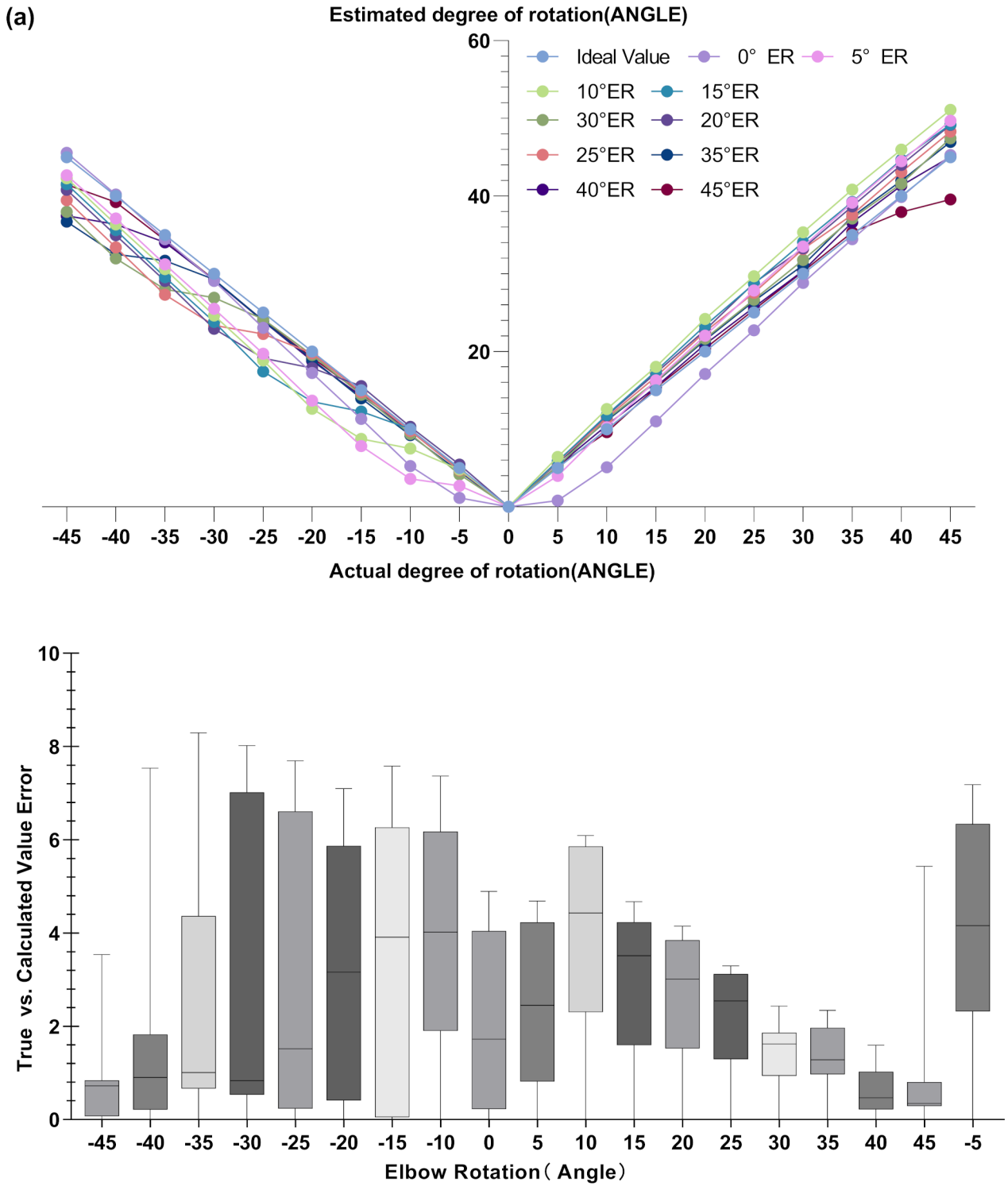

Fig. 5 (**a**) Measurements using the modified rotation correction formula (MRCF) at various degrees of elbow rotation (ER). The ideal value represents the estimated degree of rotation equal to the actual degree. Positive values on the X-axis represent internal rotation, while negative values indicate external rotation. (**b**) Box plots illustrating the differences between measured and actual values for various degrees of elbow rotation using MRCF

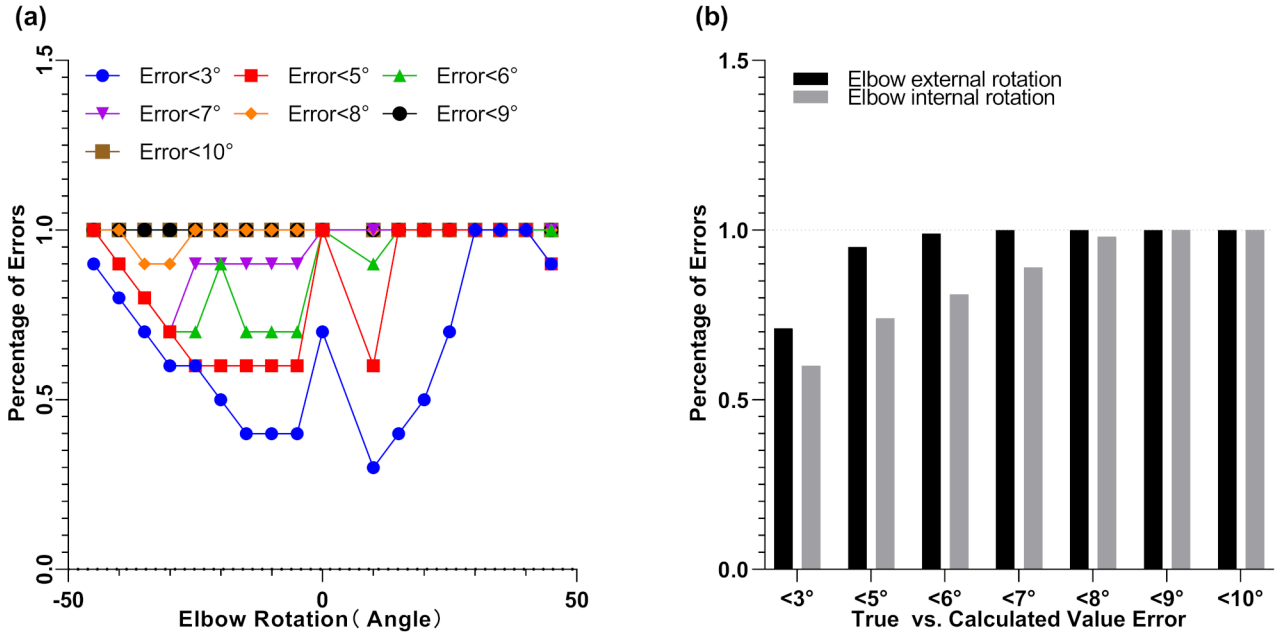

Fig. 6 (**a**) Percentage error at varying degrees of elbow rotation, calculated using the modified rotation correction formula (MRCF). (**b**) Overall percentage distribution of error levels across all measurement groups, based on MRCF calculations

reduces the error range to within 3–10°, significantly enhancing measurement precision and minimizing the rotational displacement errors caused by changes in elbow position.

In the initial modified method, we used AP view as the measurement plane. However, we found that due to the asymmetry of the distal humerus, when the elbow or fragment externally rotates by 5°-10°, the measured width of the fracture line in the horizontal plane is greater than that in the standard position, resulting in an MRCF ratio greater than 1, which prevents accurate calculation of the true rotational displacement. To address this issue, we then employed the lateral view as the measurement plane, effectively avoiding this problem.

To the best of our knowledge, this method offers a superior approach to assessing rotational displacement compared to previous studies. This research is the first to highlight the potential impact of elbow rotation on the accuracy of existing rotational displacement assessment formulas. Additionally, we innovatively applied Mimics software to reconstruct the humeral supracondylar fracture model and simulate fluoroscopy in our experiment.

In 1962, Lonroth et al. attempted to assess rotational displacement by taking multiple X-ray images of the humerus at the fracture level from different fluoroscopic angles [19]. However, the repeated fluoroscopy used in this method increased radiation exposure to children. In 2001, Gordon introduced the concept of LRP, which indirectly reflects the rotational changes before and after the healing of SCHF by calculating the percentage of the absolute difference in width between the distal and proximal fracture fragments and the width of the distal fracture fragment [15]. However, LRP does not directly quantify the degree of rotational displacement.

To further investigate the relationship between LRP and true rotational displacement, Berdis and Şahbat built upon Lonroth's approach, using linear regression analysis to demonstrate a positive correlation between LRP and true rotational displacement across various fracture models [18, 20]. In addition, Prabhaker et al. developed a mathematical model for assess the degree of rotational displacement at the fracture site [14]. They demonstrated that when this model was applied to 3D-printed fracture models, more than 75% of the measurements had an error of less than 5° compared to the true values. This approach reduced errors introduced by manual adjustments by using software modeling and 3D printing to generate fracture models with varying degrees of rotational displacement.

In contrast to their work, our modified rotational calculation formula offers a more direct assessment of the true degree of rotational displacement by incorporating the effects of elbow rotation. Additionally, we used Mimics software to simulate X-ray fluoroscopy, enabling clear identification of anatomical landmarks at the distal humerus in the simulated images. This digital fluoroscopy simulation allows for adjustable settings of elbow rotation and the relative rotational displacement between the distal and proximal bone fragments. The clear simulated fluoroscopic images provide a reliable foundation

for further validation of the method's accuracy, while the adjustable simulation minimizes errors from manual adjustments. This approach also reduces radiation exposure from repeated fluoroscopy, offering a feasible solution for extensive simulation requirements.

In addition to fluoroscopic methods, CT and non-invasive ultrasound technology have also been used to assess rotational displacement in SCHF. Hindman and colleagues used CT cross-sectional scans to calculate the rotational angle difference between the fractured and normal bone segments, thus determining the true rotational displacement [21]. Ito and colleagues attempted to use ultrasound, adding two measurement points to the original protocol by measuring the distance from the medial and lateral humeral columns to the skin, in order to assess rotational displacement [22]. However, this method does not quantify rotational displacement.

Although ultrasound and spiral CT have improved the accuracy of detecting rotational displacement, intraoperative C-arm fluoroscopy remains the most commonly used and convenient clinical method. Henderson's method has provided a solid foundation for our subsequent research, which is based on conventional fluoroscopy.

However, our study does have the following limitations: (1) Complexity of MRCF: The MRCF method is relatively complex and may not be conducive to direct and rapid evaluation in a clinical setting; (2) Reference Requirements: The MRCF method requires the width of the fracture line fragments in AP and lateral views of the humerus in a non-rotated state as references for calculating rotation; (3) Simulation Constraints: Our study only simulated transverse fractures and rotational displacement centered around the humeral axis. In real-world scenarios, fracture lines may be more complex, and rotational displacement can occur around different axes [23]; (4) Effect of Fracture Level: Consistent with previous studies, the higher the fracture level, the more circular the humeral shape becomes, which reduces the accuracy of rotational displacement evaluation; (5) Experience-Dependent Assessment: The MRCF method requires determination of the rotation direction of the bone fragments, which, in clinical practice, requires considerable experience to assess accurately.

To address these limitations, we propose several potential solutions. First, to facilitate clinical application, we have developed an online calculation tool [24]. By simply entering the relevant fluoroscopic measurement parameters, clinicians can quickly and directly assess the degree of rotational displacement. Second, to obtain the necessary AP and lateral views of the humerus at the fracture line level in a non-rotated state, the contralateral limb can be used for fluoroscopy. Unlike adjusting the affected limb, the healthy limb can achieve the necessary fluoroscopic position, thus providing relatively standardized images. Third, the MRCF method, which compares the pre- and post-rotation changes in bone fragment widths on lateral views, is applicable to various types of non-high fractures of SCHF. Finally, to ensure consistent determination of rotational direction during fluoroscopy, the C-arm angle can be adjusted as needed to standardize the rotation direction of the bone fragments.

We believe our study provides a reliable and clinically applicable method that effectively addresses the limitations of previous research. It offers a relatively accurate quantification of rotational displacement based on fluoroscopy, even when considering both internal and external elbow rotation. Previous studies have shown that poor residual rotational displacement is associated with complications such as ulnar nerve neuropathy and cubitus varus deformity [9–12]. With the increased accuracy and convenience of MRCF in assessing residual rotational displacement, this method enhances physicians' attention to residual displacement, supporting more informed clinical decisions. Ultimately, it may help reduce the occurrence of unacceptable residual rotational displacement following closed reduction, thereby lowering the incidence of complications associated with poor rotational alignment and improving the overall prognosis of pediatric humeral supracondylar fractures.

Future work will focus on applying the modified rotational calculation formula in clinical practice to establish the acceptable degree of postoperative rotational displacement. Additionally, efforts will be directed toward integrating the latest artificial intelligence technologies to further enhance the accuracy and convenience of the assessment method.

Conclusions

This study demonstrates that the accuracy of PRCF decreases as the degree of elbow rotation increases, which aligns with our initial hypothesis. In contrast, MRCF effectively addresses the limitations of PRCF, providing a more stable and accurate measurement of rotational displacement, even under varying degrees of elbow rotation. The use of MRCF, in conjunction with the online calculator, enhances its practical application and serves as a valuable tool for accurately assessing the relationship between residual rotational displacement in pediatric humeral supracondylar fractures and the risk of poor outcomes.

Abbreviations

SCHF Supracondylar Humerus Fractures
LRP Lateral Rotation Percentage

PRCF	The Primitive Rotational Calculation Formula
MRCF	The Modified Rotational Calculation Formula
3D	Three-Dimensional
CT	Computed Tomography
AP	Anterior-Posterior
ICC	Intraclass Correlation Coefficient

Acknowledgements
Not applicable.

Author contributions
Yong Liu and Qiang Jie conceptualized and designed the study. Yong Liu, Jianping Sun, Jining Qu, Bohai Qi, and Yating Yang collected and analyzed the data. Yong Liu, Xiaoju Liang, and Qiang Jie wrote the manuscript. All authors read and approved the final manuscript.

Funding
This work was supported by a grant from the Innovation Capability Support Program of Shaanxi Province (Grant No. 2024SF-LCZX-16) and the Shaanxi Province Health Scientific Research Innovation Ability Promotion Plan (Grant No. 2024PT-12).

Data availability
The datasets used and/or analyzed during the current study are available from the corresponding author on reasonable request.

Declarations

Ethics approval and consent to participate
The study was approved by the Clinical Research Ethics Committee of the Xi'an Jiaotong University Affiliated Honghui Hospital (style no.202407001). Written informed consent was obtained from all parents or legal guardians of participants under the age of 16 prior to their participation in the study. All procedures were conducted in accordance with relevant guidelines and regulations, following the Declaration of Helsinki.

Consent for publication
All parents or legal guardians of participants under the age of 16 provided written informed consent for the publication of identifying images and clinical data.

Competing interests
The authors declare no competing interests.

Author details
[1]Pediatric Orthopedic Hospital, Honghui Hospital, Xi'an Jiao tong University, Xi'an 710000, China
[2]Research Center for Skeletal Developmental Deformity and Injury Repair, School of Life Science and Medicine, Northwest University, Xi'an 710000, China
[3]Yan'an University School of Medicine, Yan'an 716099, China

Received: 15 September 2024 / Accepted: 23 December 2024
Published online: 06 January 2025

References

1. Cheng JCY, Lam TP, Maffulli N. Epidemiological features of supracondylar fractures of the humerus in Chinese children. J Pediatr Orthop Part B. 2001;10:63–7.
2. Vaquero-Picado A, González-Morán G, Moraleda L. Management of supracondylar fractures of the humerus in children. EFORT Open Reviews. 2018;3:526–40.
3. Gamble JG, Vorhies JS. Remodeling of sagittal plane malunion after pediatric supracondylar humerus fractures. J Pediatr Orthoped. 2020;40:e903.
4. Kim YK, Lee SH. Age-dependent sagittal plane remodeling of pediatric supracondylar fractures. J Pediatr Orthoped. 2024;44:407.
5. Miyake T, Miyamura S, Miki R, Shiode R, Iwahashi T, Kazui A, et al. Cubitus varus deformity following paediatric supracondylar humeral fracture remodelling predominantly in the sagittal direction: a three-dimensional analysis of eighty-six cases. Int Orthop. 2024. https://doi.org/10.1007/s00264-024-06197-2.
6. Persiani P, Di Domenica M, Gurzi M, Martini L, Lanzone R, Villani C. Adequacy of treatment, bone remodeling, and clinical outcome in pediatric supracondylar humeral fractures. J Pediatr Orthop B. 2012;21:115–20.
7. Sanpera I, Salom M, Fenandez-Ansorena A, Frontera-Juan G, Pizà-Vallespir G. The fate of the malrotated elbow supracondylar fractures in children: is varus really a problem? Int Orthop. 2024;48:1453–61.
8. Seo KB, Kim BS, Park Y-G, Lim C. Associated factor and long-term clinical outcomes for patients with postoperative rotational malreduction in Pediatric Supracondylar Humeral fractures. Med (Kaunas). 2024;60:791.
9. Flierl MA, Carry PM, Scott F, Georgopoulos G, Hadley-Miller N. Rotation and displacement predict adverse events in pediatric supracondylar fractures. Orthopedics. 2015;38.
10. Gedikbaş M. Does rotational deformity cause poor outcomes after pediatric supracondylar humerus fractures? Turk J Trauma Emerg Surg. 2023;29:811–7.
11. Mitsunari A, Muneshige H, Ikuta Y, Murakami T. Internal rotation deformity and tardy ulnar nerve palsy after supracondylar humeral fracture. J Shoulder Elb Surg. 1995;4:23–9.
12. Wang Y, Chong Q, Zhang S, Ben Y, Li Q, Chen D et al. Analysis of risk factors for failed closed reduction in pediatric gartland type III supracondylar humerus fracture. J Shoulder Elb Surg. 2024;:S1058-2746(24)00409-9.
13. Henderson ER, Egol KA, Van Bosse HJP, Schweitzer ME, Pettrone SK, Feldman DS. Calculation of rotational deformity in pediatric supracondylar humerus fractures. Skeletal Radiol. 2007;36:229–35.
14. Prabhakar P, Pierce WA, Standefer KD, Ho CA. Can we estimate the amount of malrotation in supracondylar humerus fractures after CRPP? J Orthop Trauma. 2020;34:e245–9.
15. Gordon JE, Patton CM, Luhmann SJ, Bassett GS, Schoenecker PL. Fracture stability after pinning of displaced supracondylar distal humerus fractures in children. J Pediatr Orthoped. 2001;21:313–8.
16. Müller SA, Adolfsson L, Baum C, Müller-Gerbl M, Müller AM, Rikli D. Fluoroscopy of the elbow: a cadaveric study defining new standard projections to visualize important anatomical landmarks. JBJS Open Access. 2021;6.
17. Omid R, Choi PD, Skaggs DL. Supracondylar humeral fractures in children. J Bone Joint Surgery-American Volume. 2008;90:1121–32.
18. Berdis G, Hooper M, Talwalkar V, Walker J, Muchow R, Riley S, et al. Assessment of lateral rotation percentage and rotational deformity of the elbow in type 3 supracondylar humerus fractures: a biomechanical study. J Pediatr Orthoped. 2021;41:e605–9.
19. Lonroth H. Measurement of rotational displacement in supracondylar fractures of the humerus. Acta Radiol. 1962;57:65–70.
20. Şahbat Y, Baysal Ö, Ağırdil Y, Polat M, Büyüktopçu Ö, Shammadli Z, et al. Is radiological rotation measurement affected by the fracture pattern in pediatric supracondylar humeral fractures? Acta Radiol. 2023;64:2748–56.
21. Hindman BW, Schreiber RR, Wiss DA, Ghilarducci MJ, Avolio RE. Supracondylar fractures of the humerus: prediction of the Cubitus varus deformity with CT. Radiology. 1988;168:513–5.
22. Ito N, Eto M, Maeda K, Rabbi ME, Iwasaki K. Ultrasonographic measurement of humeral torsion. J Shoulder Elb Surg. 1995;4:157–61.
23. Bahk MS, Srikumaran U, Ain MC, Erkula G, Leet AI, Sargent MC, et al. Patterns of pediatric supracondylar humerus fractures. J Pediatr Orthoped. 2008;28:493–9.
24. The Rotary-Calculator. https://lauyo.github.io/rotary-calculator.github.io/.Accessed 15 Sept 2024.

Publisher's note